星形成ゼミ 2024/10/18 #GAEP 0927-1003 68-134

辰馬 (理研iTHEMS)

arXiv:2409.19204
ATOMS: ALMA Three-millimeter Observations of Massive Star-forming regions – XVII. High-mass star-formation through a large-scale collapse in IRAS 15394−5358
Das et al.

arXiv:2409.18793
Giant planets population around B stars from the first part of the BEAST
Delorme et al.

ATOMS: ALMA Three-millimeter Observations of Massive Star-forming regions – XVII. High-mass star-formation through a large-scale collapse in IRAS 15394−5358

- ハブフィラメント系: 大質量星形成の場。
- ALMAによる大質量protoclusterのdust continuum (3 mm)と分子輝線の観測。
- 843 M_{sun}のclumpは6つのコアに分裂していることがわかった。
- C-1Aが最も大きく(半径0.04 pc)、最も重く(157 M_{sun})、密度の高い中心領域にある。7, 3 M_{sun}のコアも近くにある。
- 分裂仮定はthermal Jeans分裂と一致。
- 全てのコアは重力的に束縛されている(ビリアルパラメータα_{vir} << 2)
- 質量-半径の関係より、3つのコアは大質量星を形成しうる。
- $H^{13}CO^+$の積分強度図より、大質量clumpはハブフィラメント系(中心のハブが4つのフィラメントとつながっている)と関連している。
- ハブに向かう鋭い速度勾配が観測されており、フィラメントが活発的にハブに質量を与えていることが示唆される。

ABSTRACT

Hub-filament systems are considered as natural sites for high-mass star formation. Kinematic analysis of the surroundings of hub-filaments is essential to better understand high-mass star formation within such systems. In this work, we present a detailed study of the massive Galactic protocluster IRAS 15394−5358, using continuum and molecular line data from the ALMA Three-millimeter Observations of Massive Star-forming Regions (ATOMS) survey. The 3 mm dust continuum map reveals the fragmentation of the massive (M = 843 $M_\odot$) clump into six cores. The core C-1A is the largest (radius = 0.04 pc), the most massive (M = 157 $M_\odot$), and lies within the dense central region, along with two smaller cores (M = 7 and 3 $M_\odot$). The fragmentation process is consistent with the thermal Jeans fragmentation mechanism and virial analysis shows that all the cores have small virial parameter values ($\alpha_{vir} << 2$), suggesting that the cores are gravitationally bound. The mass vs. radius relation indicates that three cores can potentially form at least a single massive star. The integrated intensity map of $H^{13}CO^+$ shows that the massive clump is associated with a hub-filament system, where the central hub is linked with four filaments. A sharp velocity gradient is observed towards the hub, suggesting a global collapse where the filaments are actively feeding the hub. We discuss the role of global collapse and the possible driving mechanisms for the massive star formation activity in the protocluster.

ATOMS: ALMA Three-millimeter Observations of Massive Star-forming regions – XVII. High-mass star-formation through a large-scale collapse in IRAS 15394−5358

- IRAS 15394−5358: 1.8 kpcに位置するprotocluster
  - 質量843.3 M_{sun}、半径0.5 pc、ダスト温度20.7 K、光度5.4 x 10^3 L_{sun}のa single dust clump (870 μm)

赤: 24 μm、緑: 8 μm

赤: 8 μm、緑: 4.5 μm、青: 3.6 μm

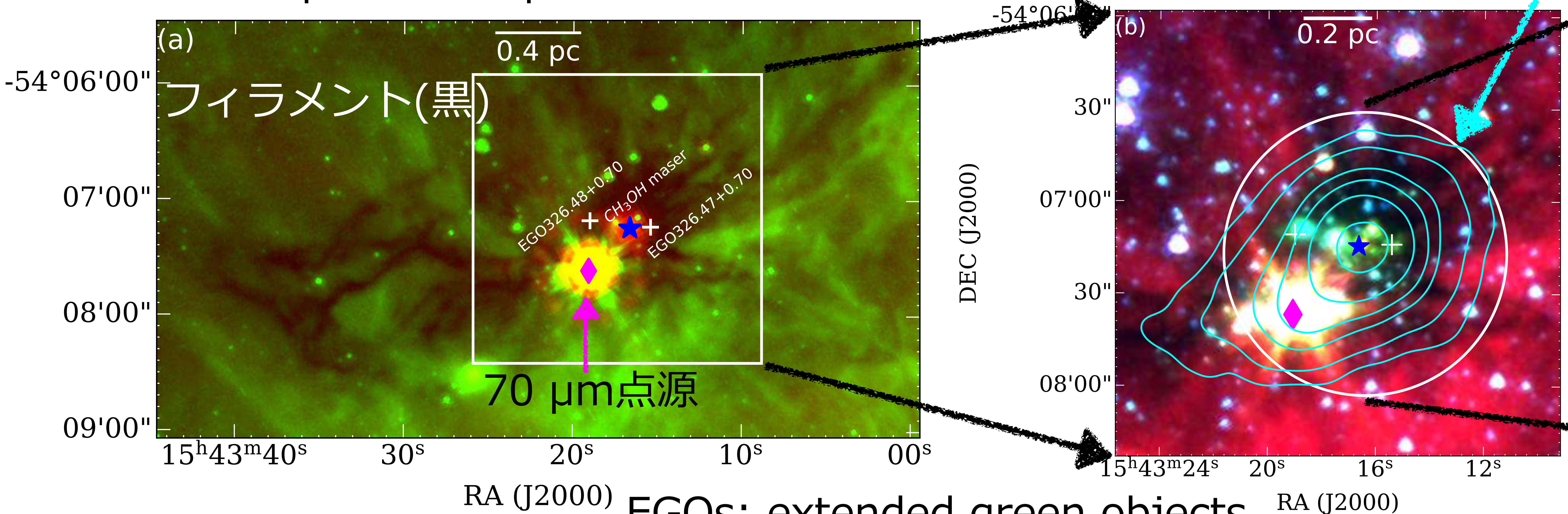

EGOs: extended green objects

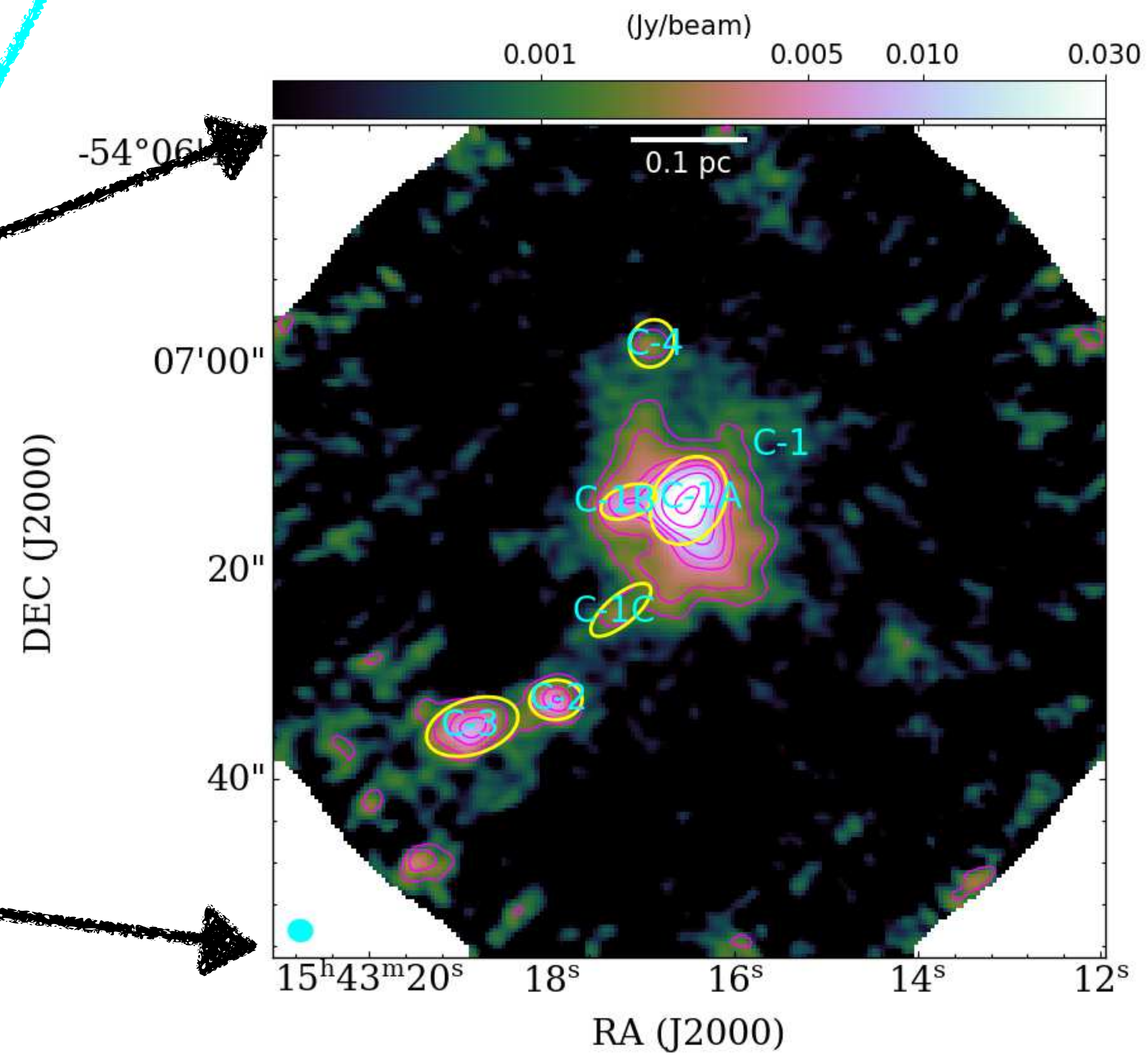

赤紫: 3 mm、黄: コア

Figure 1. (a) Two color composite image (24 μm - red and 8 μm - green) of the region towards IRAS 15394−5358. This image shows a larger field of view of the surrounding area of the star-forming region, which lie on the large IRDC. The white box covers a close region around IRAS 15394−5358. (b) Three color-composite image (8 μm - red, 4.5 μm - green, and 3.6 μm - blue) of the white box region shown in (a). The white circle (radius = 0.7′) is the ALMA field of view. The cyan contours are emissions at 870 μm from the ATLASGAL survey. The contour levels are 0.6, 1, 2, 3, 5, and 10 Jy/beam. Different objects towards the region found in the literature are shown in different symbols. The white '+' marks are for the EGOs (Cyganowski et al. 2008), the blue star shows the location of 6 GHz CH_3OH maser (Caswell 1998), and the magenta diamond for the position of the 70 μm point source. Scale bars of both images are shown on top of each frame.

Figure 2. The 3 mm continuum map of the protocluster observed as part of the ATOMS survey is shown in colour. The magenta contours are from the same map with contour levels of 3, 5, 10, 15, 25, and 50 times the noise σ, where σ = 0.0004 Jy/beam. The yellow ellipses, along with labels, are the identified cores. A scale bar of 0.1 pc is shown on the top, and the beam size is in the bottom left corner.

ATOMS: ALMA Three-millimeter Observations of Massive Star-forming regions – XVII. High-mass star-formation through a large-scale collapse in IRAS 15394−5358

- 3 mmのdust continuumより、clumpは6つのコアに分裂していることがわかった。
    - 密度の高い中心領域は214 M_{sun}で、C-1A, C-1B, C-1Cの3つのコアに分かれている。
    - C-1Aが最も大きく重く密度が高い(半径0.04 pc、157 M_{sun}、8.6 g cm^{-2})

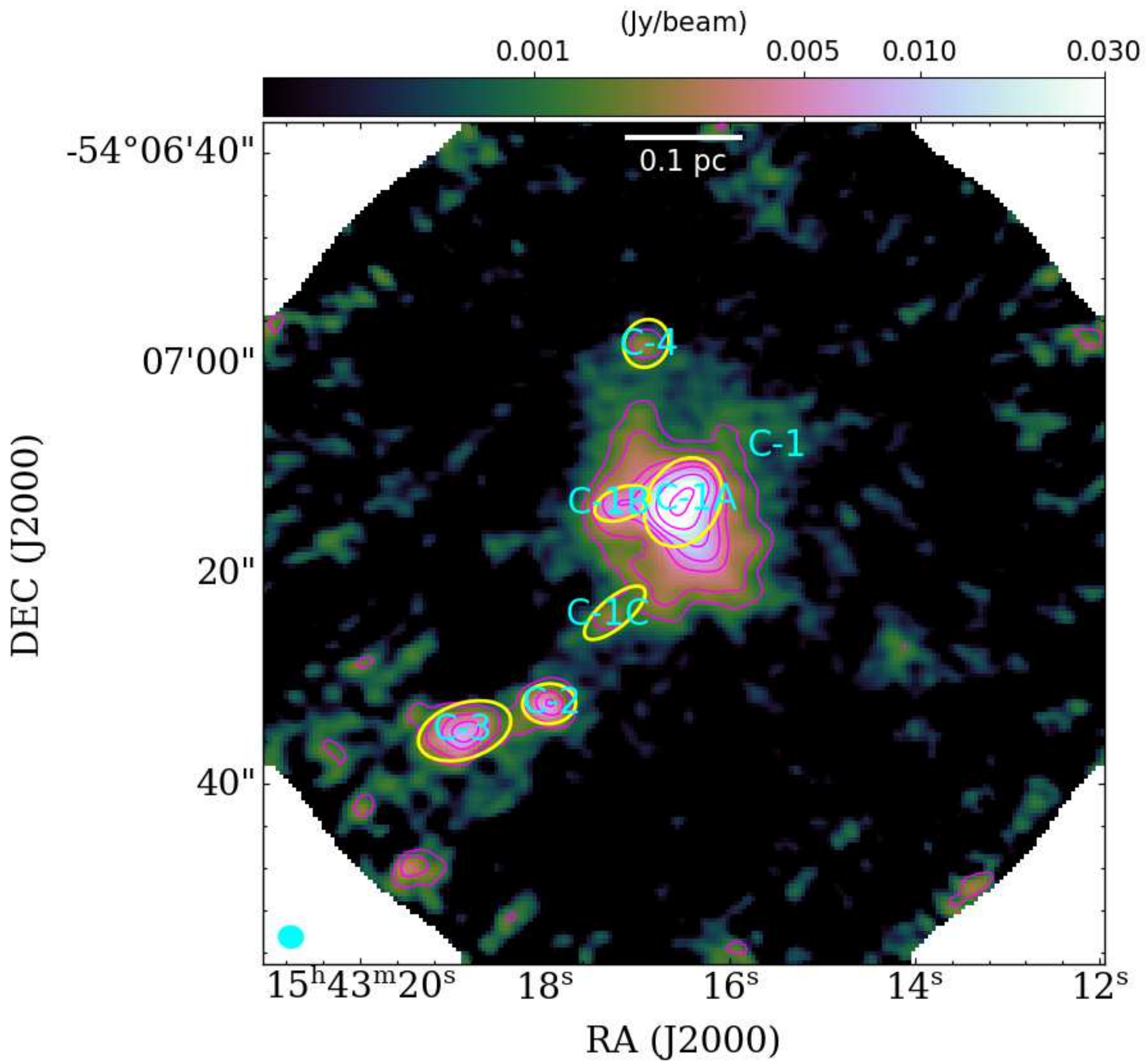

赤紫: 3 mm、黄: コア

$$\Sigma_{\rm core} = M_{\rm core}/\pi R_{\rm core}^2$$

Name	V_{LSR} (km/s)	T_d (K)	R_{core} (pc)	M_{core} ($M_\odot$)	Σ_{core} (g cm^{-2})	α_{vir}
C-1A	-40.0 ± 3.0	23.5±0.4 (39.1±0.02)	0.04	271±155 (157±90)	14.8±8.5 (8.6±4.9)	0.07 (0.12)
C-1B	-42.4 ± 1.3	23.5±0.4 (39.1±0.02)	0.02	12±7 (7±4)	2.4±1.4 (1.5±0.8)	0.54 (0.93)
C-1C	-42.6 ± 0.9	23.5±0.4 (39.1±0.02)	0.02	6±3.5 (3.4±2.1)	0.9±0.5 (0.6±0.3)	0.01 (0.01)
C-2	-42.6 ± 0.1	25.1±0.5	0.02	17±10	2.9±1.7	0.35
C-3	-42.0 ± 7.0	25.1±0.5 (46.8±0.1)	0.03	34±19.5 (17.5±10)	2.4±1.4 (1.2±0.7)	0.49 (0.94)
C-4	-41.5 ± 0.1	19.5±0.8	0.03	9±5	0.9±0.5	0.30

※()の値を使う

$$M_{\rm core} = \frac{F_\nu^{\rm int}\, R_{\rm gd}\, D^2}{B_\nu(T_d)\, \kappa_\nu},$$

R_{gd} = 100: ガスダスト比

κ_ν = 0.18 cm^2 g^{-1}: opacity

ATOMS: ALMA Three-millimeter Observations of Massive Star-forming regions – XVII. High-mass star-formation through a large-scale collapse in IRAS 15394−5358

- ビリアル分析によると、

全てのコアは重力的に

束縛されている。

$$\alpha_{\rm vir} = \frac{5\sigma_{\rm v}^2 R_{\rm core}}{G M_{\rm core}},$$ σ$_v$: 速度分散

Name	$\alpha_{\rm vir}$
C-1A	0.07 (0.12)
C-1B	0.54 (0.93)
C-1C	0.01 (0.01)
C-2	0.35
C-3	0.49 (0.94)
C-4	0.30

※ $\alpha_{\rm vir} \leqslant 2$

なら重力崩壊をする

- 分裂過程

Table 3. Density of clump and derived Jeans parameters.

ρ (g cm^{-3})	$\lambda^{\rm Th}_{\rm Jeans}$ (pc)	$M^{\rm Th}_{\rm Jeans}$ ($M_\odot$)	$\lambda^{\rm Turb}_{\rm Jeans}$ (pc)	$M^{\rm Turb}_{\rm Jeans}$ ($M_\odot$)
1.4×10^{-19}	0.16	4.4	0.30	28.0

$$\lambda_J = \sigma_{\rm th}\left(\frac{\pi}{G\rho}\right)^{1/2} \text{ and } M_J = \frac{\pi^{5/2}}{6}\frac{\sigma_{\rm th}^3}{\sqrt{G^3\rho}},$$

$$\sigma_{\rm th} = \left(\frac{k_B T_{\rm kin}}{\mu m_H}\right)^{1/2},$$

$$\sigma_{\rm tot} = (\sigma_{\rm nt}^2 + \sigma_{\rm th}^2)^{1/2}, \quad \sigma_{\rm nt} = \sqrt{\sigma_{\rm line}^2 - \frac{k_B T_{\rm kin}}{m_{\rm line}}},$$

$$\lambda_{\rm obs} < \lambda^{\rm Th}_{\rm Jeans} < \lambda^{\rm Turb}_{\rm Jeans}$$

$$M^{\rm Th}_{\rm Jeans} < M_{\rm obs} < M^{\rm Turb}_{\rm Jean}$$

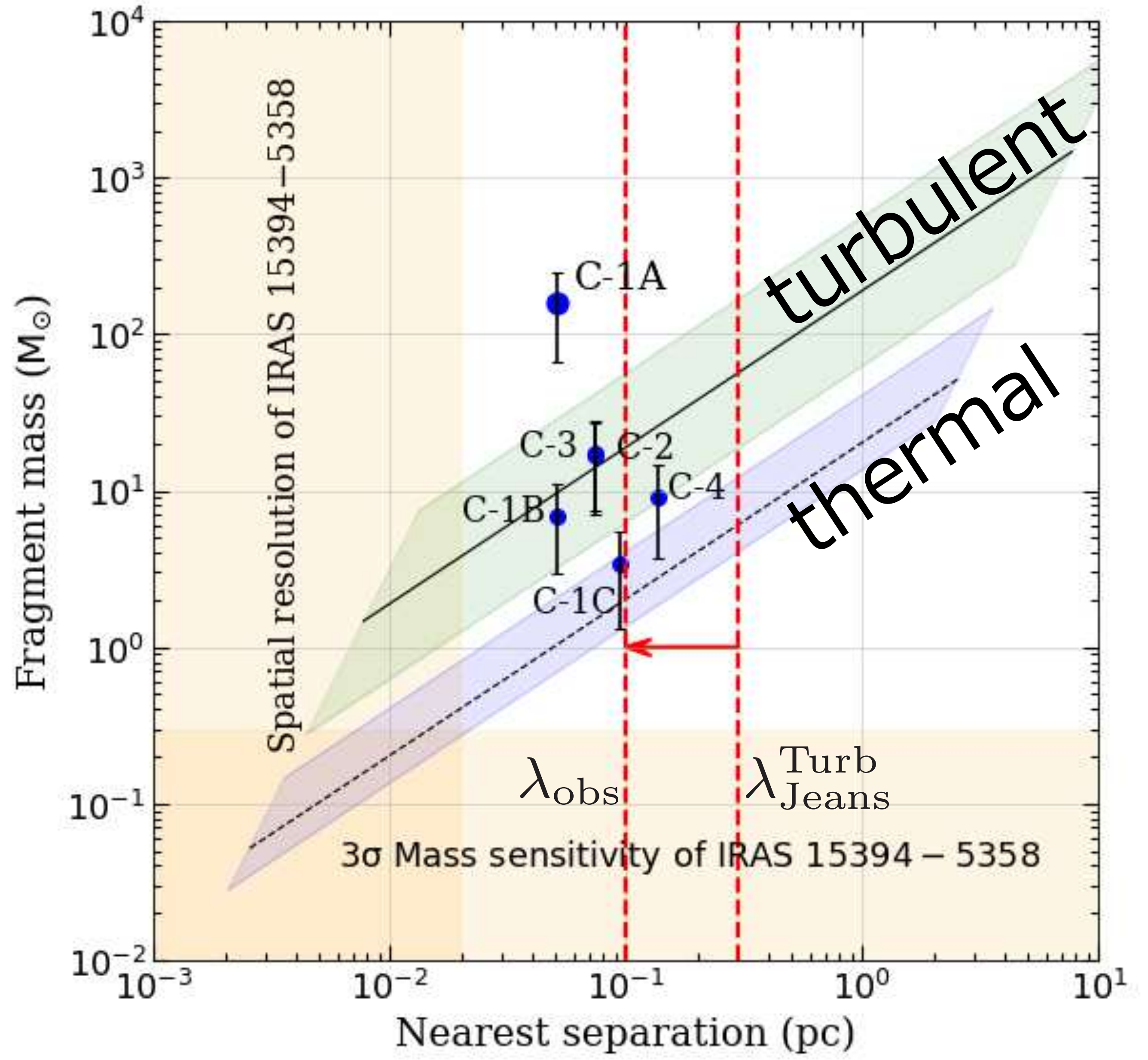

Figure 14. Fragment mass vs. the nearest separation. Here, the fragment masses are the core masses. The blue-filled circles represent the associated cores of IRAS 15394−5358. The dotted, solid black line and the shaded regions are plotted following the outlines described in Wang et al. (2014); Xu et al. (2023). Spatial and 3σ mass sensitivity of IRAS 15394−5358 with ALMA Band-3 observations is shown as an orange-shaded region. The 3σ mass sensitivity estimated using the 3σ flux density and dust temperature of 100 K. The black dotted line is for thermal Jeans fragmentation with T = 15 K and density n = [10^2, 10^8 cm^{-3}]. The blue-shaded region corresponds to the same density range, but for temperatures, T = [10, 30] K. The solid black line is for the turbulent Jeans fragmentation corresponding to velocity dispersion σ = 0.7 km s^{-1} and density n = [10^2, 10^8 cm^{-3}]. The green shaded region is for the same density but with velocity dispersion σ = [0.4, 1.2] km s^{-1}. All cores are labelled on the plot. Due to their similar masses, cores C-2 and C-3 overlap with each other. The red vertical dashed lines mark the location of 0.3 pc ($\lambda^{\rm Turb}_{\rm Jeans}$ or Jeans length assuming the cloud fragmented when its density was 10^4 cm^{-3}) and 0.1 pc, the median value of the observed core separation, respectively. The red arrow shows the length of 0.2 pc, highlighting the difference.

ATOMS: ALMA Three-millimeter Observations of Massive Star-forming regions – XVII. High-mass star-formation through a large-scale collapse in IRAS 15394−5358

- C-1A, C-2, C-3は大質量星を形成しうる。特にC-1AはO/B型星を形成する。

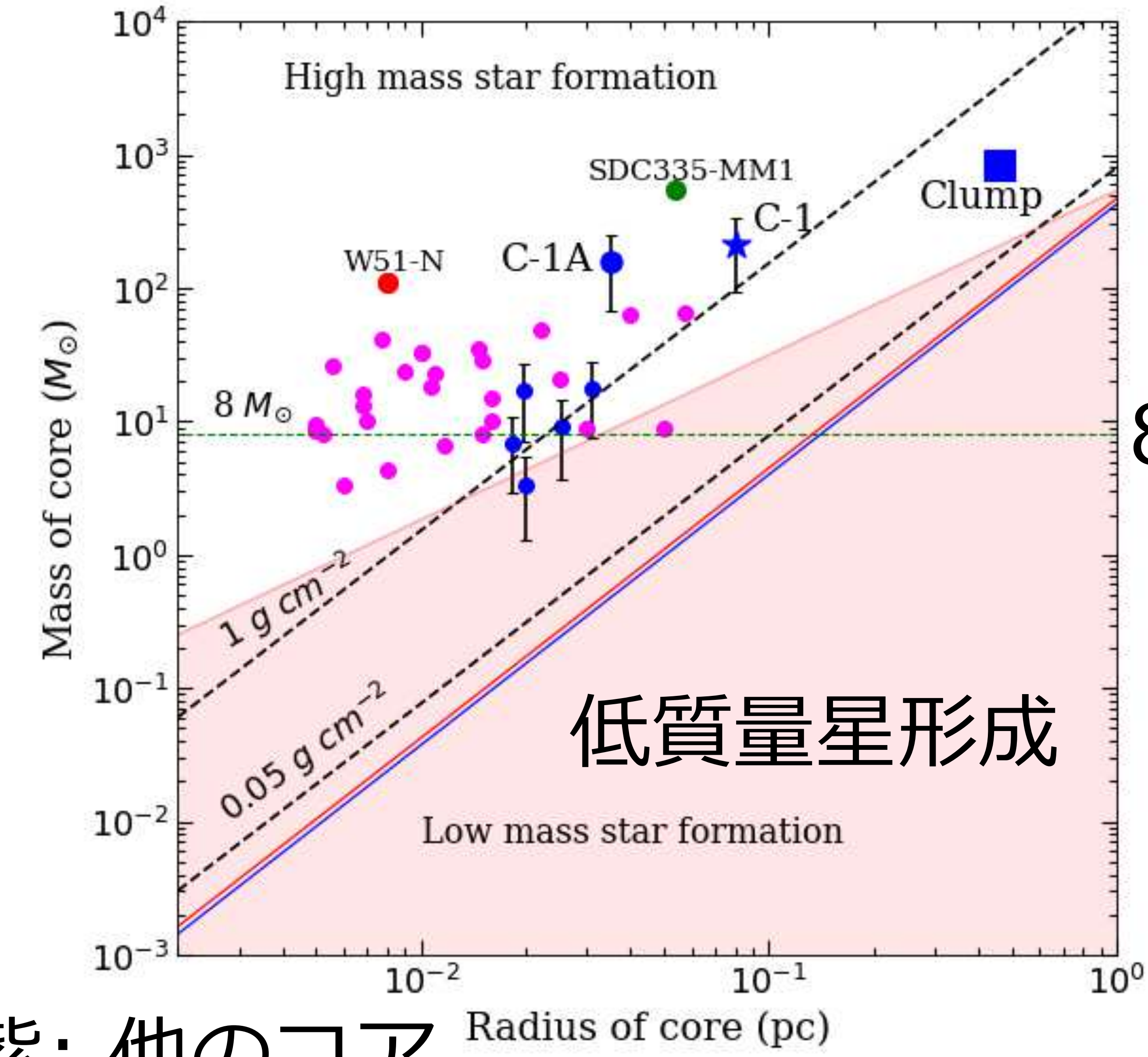

緑、赤: 他の大質量星形成コア

8 M_{sun}

赤紫: 他のコア

Figure 16. Radius vs. mass. The blue-filled circles mark the positions of the cores associated with IRAS 15394−5358. The blue-filled star and square represent the hub C-1 and the whole clump. Cores from literature (Peretto, Hennebelle & André 2007; Zapata et al. 2009; Rathborne et al. 2011; Wang et al. 2011; Peretto et al. 2013; Saha et al. 2022) are also shown in the plot as magenta-filled circles. SDC335-MM1 (Peretto et al. 2013), and W51-N (Zapata et al. 2009) are displayed as green and red-filled circles, respectively. The blue and red lines represent the surface density thresholds of 116 $M_\odot$ pc^{-2} ($\sim$ 0.024 g cm^{-2}) and 129 $M_\odot$ pc^{-2} ($\sim$ 0.027 g cm^{-2}) from Lada, Lombardi & Alves (2010) and Heiderman et al. (2010), respectively. The shaded region is for the low-mass star formation, which does not satisfy the criteria of $m(r) > 870\ M_\odot\ (r/\mathrm{pc})^{1.33}$ (Kauffmann et al. 2010). Surface density thresholds of 0.05 g cm^{-2} (Krumholz & McKee 2008), and 1 g cm^{-2} (Urquhart et al. 2014) are shown as dashed black lines. The green dashed line is for a core mass of 8 $M_\odot$.

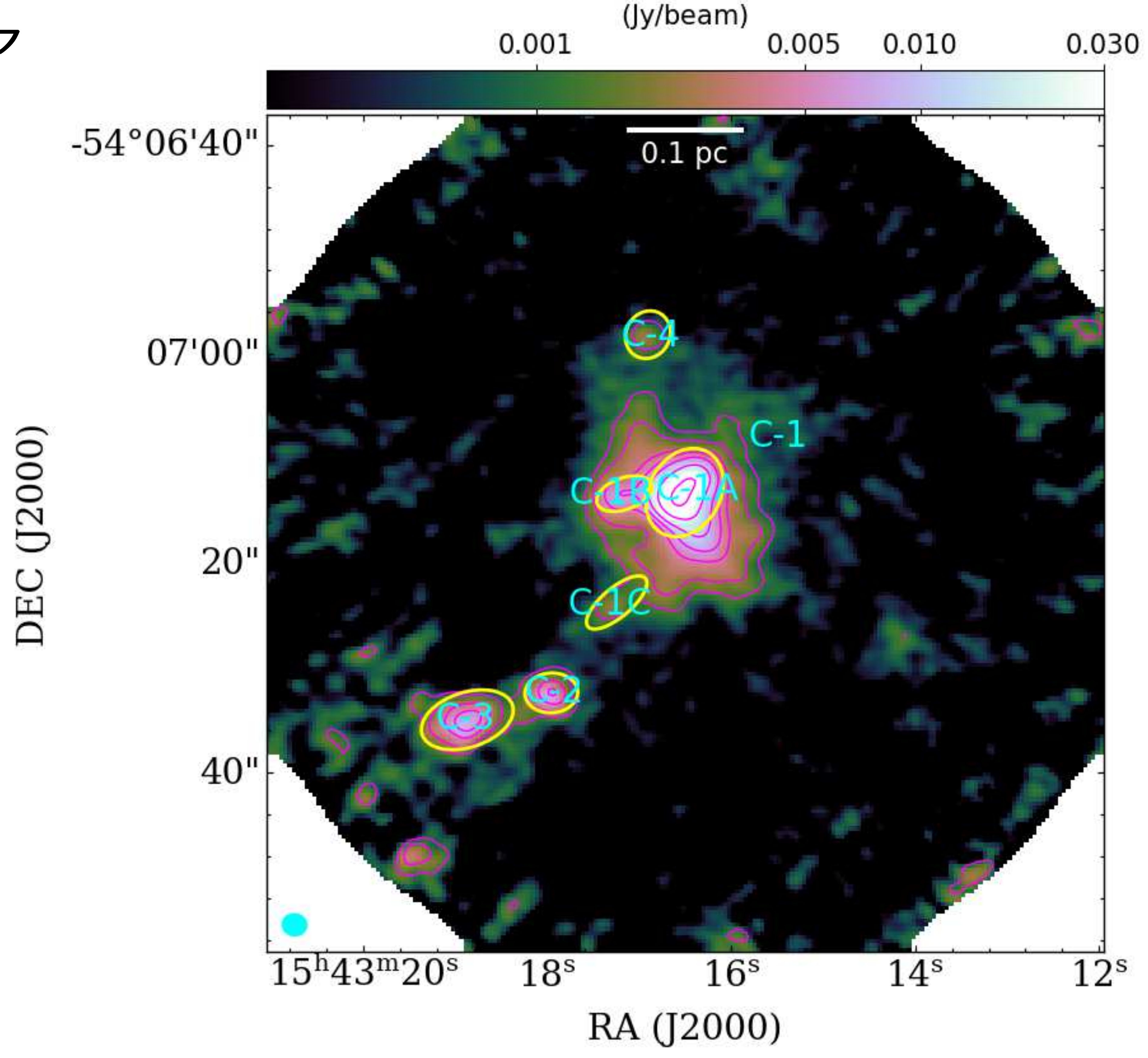

赤紫: 3 mm、黄: コア

ATOMS: ALMA Three-millimeter Observations of Massive Star-forming regions – XVII. High-mass star-formation through a large-scale collapse in IRAS 15394−5358

- $H^{13}CO^{+}$によると、中心のハブが4つのフィラメント(F1—F4)とつながっている。
  - moment 1によると、周りからハブへの速度勾配(平均~ 20 km s^{-1} pc^{-1})がある。
  - これはglobalな崩壊を示しており、F1—F4がハブにガスを流入している。

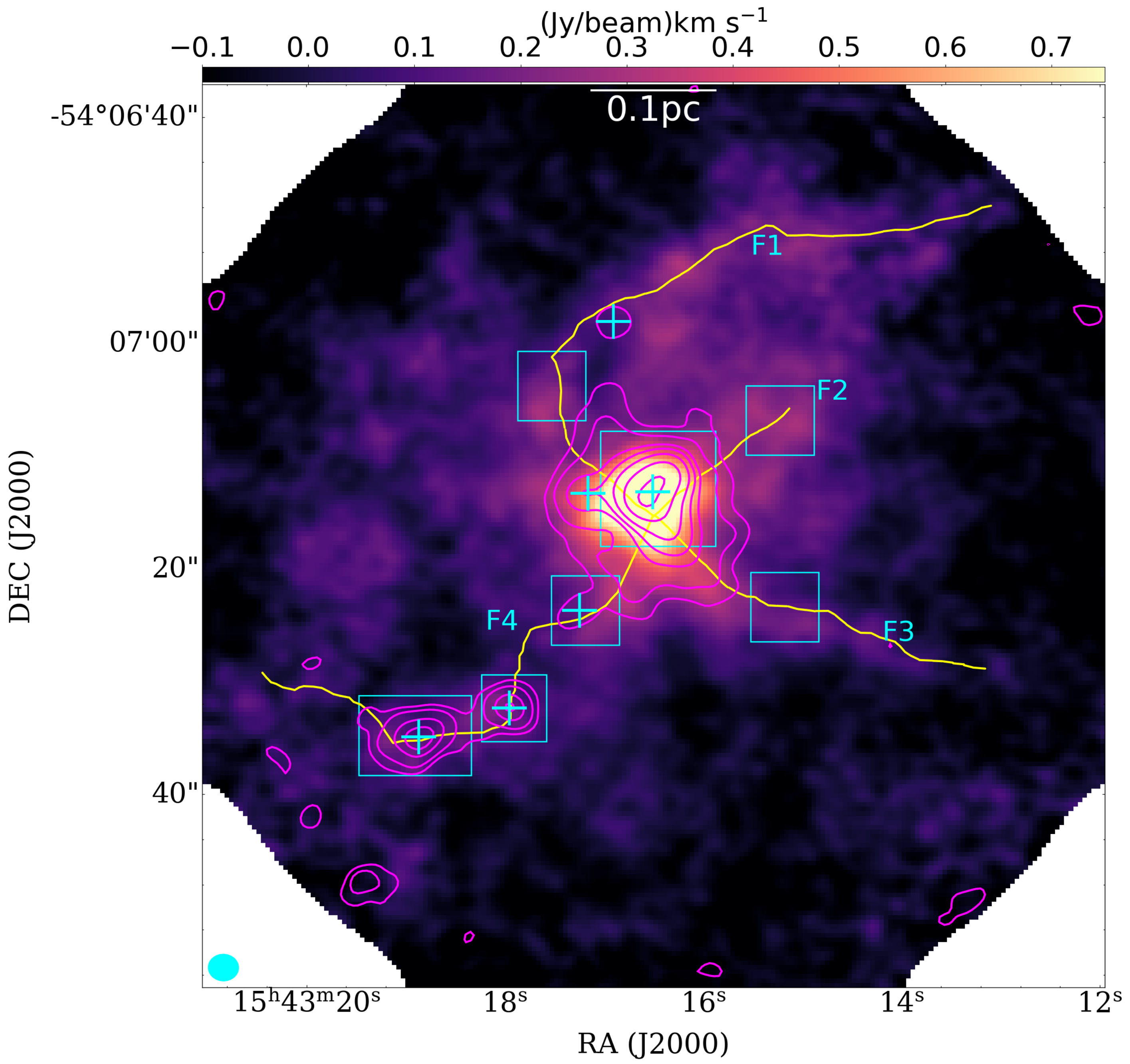

Figure 8. Integrated intensity map of $H^{13}CO^{+}$. The filaments are shown as yellow lines and labelled from F1 to F4. The 3 mm continuum emission is shown as magenta contours, with the same contour levels as of Fig. 2. The '+' marks display the locations of the identified dense cores in the region. The cyan boxes on the central core and the filaments are the regions where spectra are extracted to analyze the infall signature in that region.

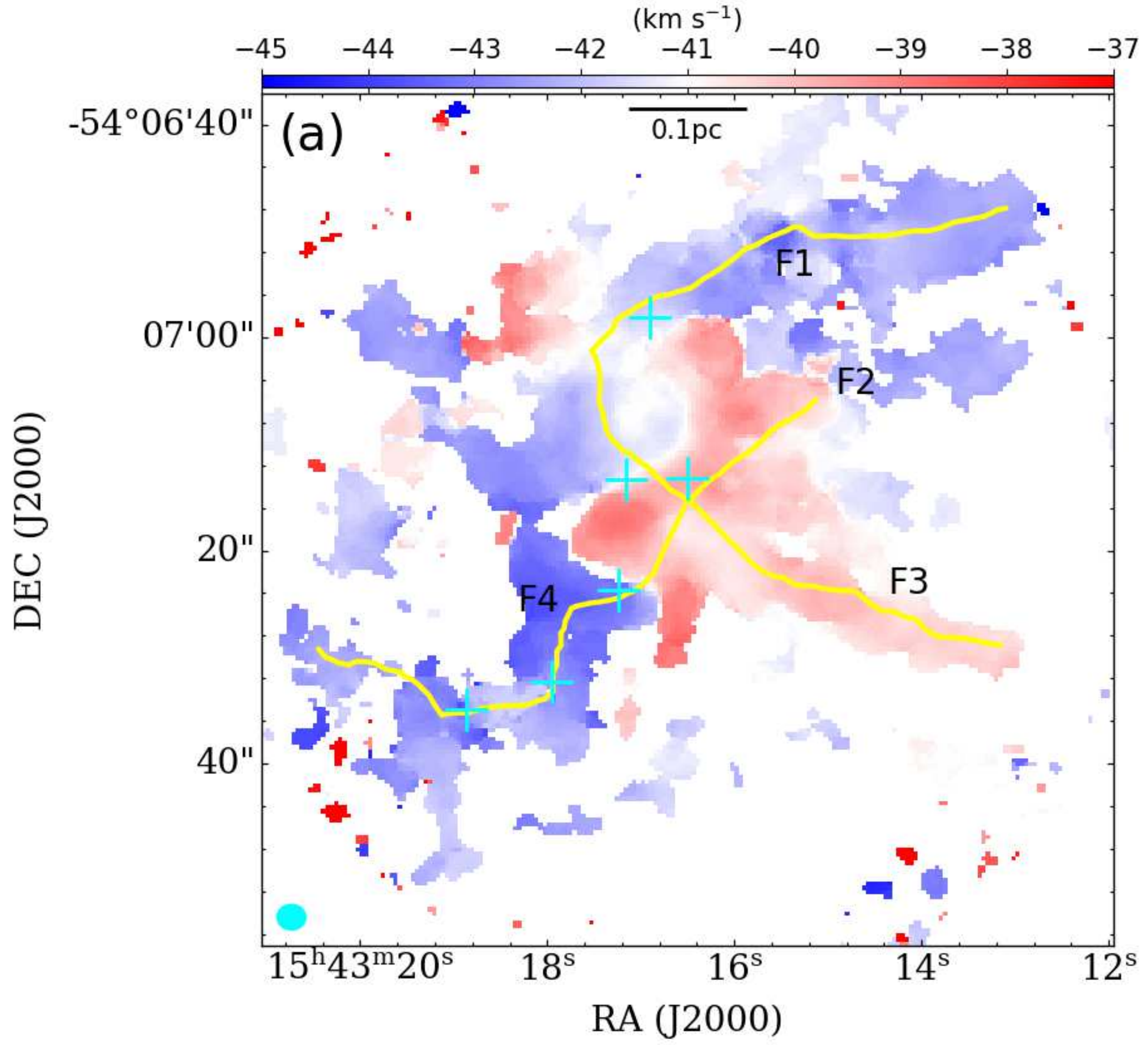

Figure 11. Moment1 (a) and moment2 (b) maps of $H^{13}CO^{+}$ line trans
The '+' marks are the locations of the dense cores. Both the mome
and considering pixels above 5σ, where σ = 0.009 Jy/beam. Scale ba

$H^{13}CO^{+}$
黄: フィラメント
赤紫: 3 mm continuum
+: コア

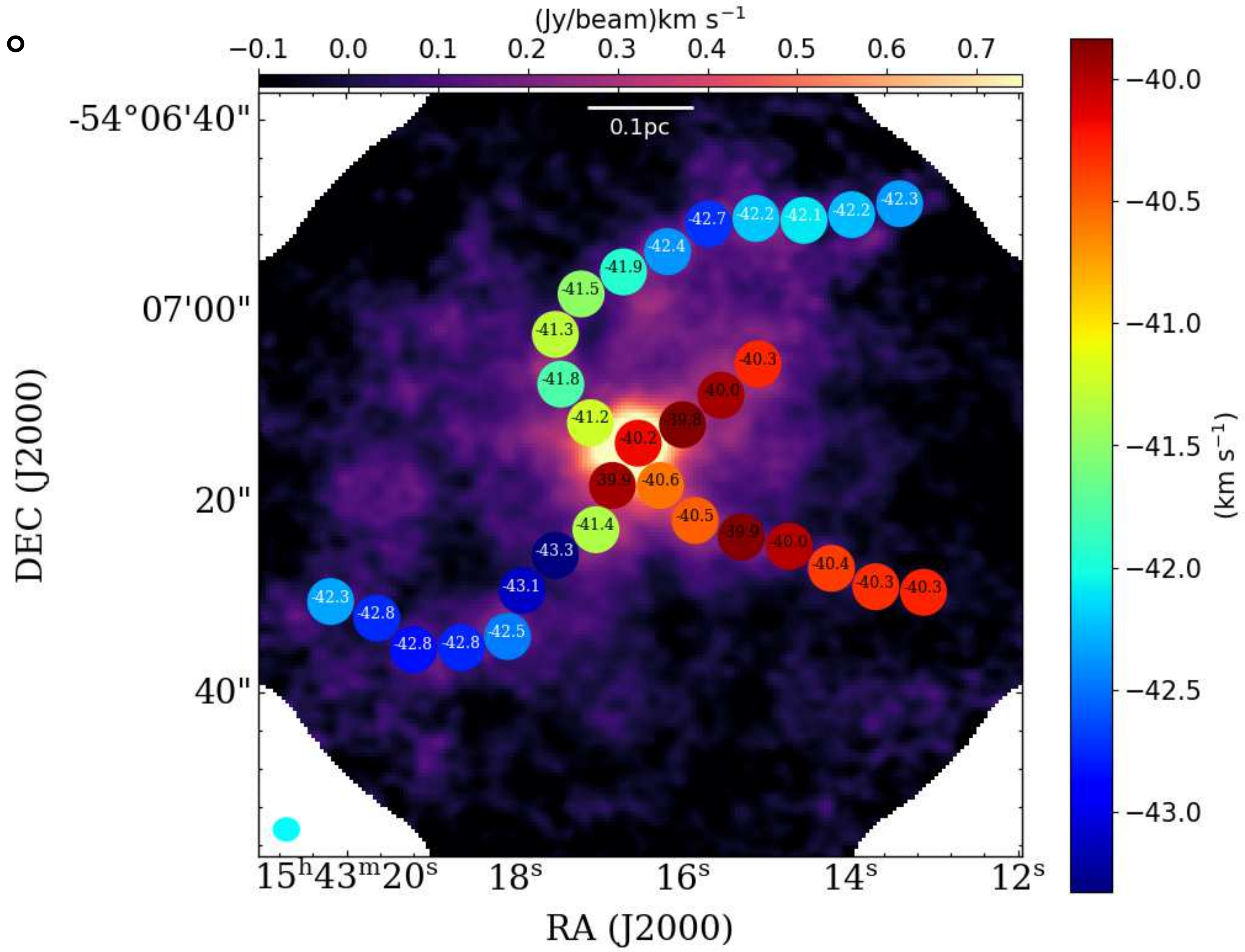

Figure 17. The background image is the moment0 map of the $H^{13}CO^{+}$ molecular line transitions. LSR velocities obtained within circular regions (2.5″), equivalent to the beam size, are overplotted on the image. The colour coding of the circles represents the variation in LSR velocities. The colour bar of the variation is also shown in the plot. The scale bar is shown on the top, and the beam size is shown in the bottom left corner.

ATOMS: ALMA Three-millimeter Observations of Massive Star-forming regions – XVII. High-mass star-formation through a large-scale collapse in IRAS 15394−5358

- $H^{13}CO^+$のmoment 2によると、ハブに向かって線幅が広がっており(~ 1.8 km s^{-1})、中心領域で星形成が活発化していることが示唆される。

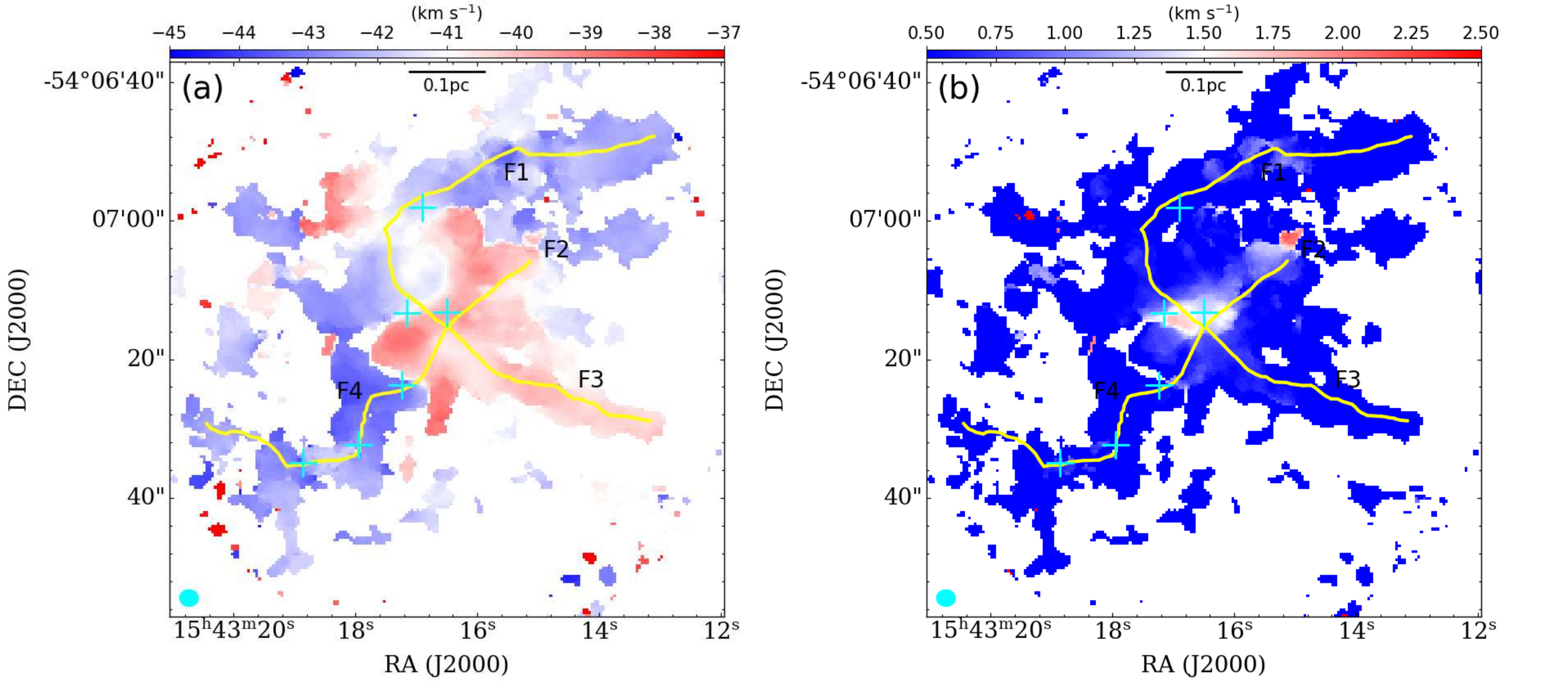

Figure 11. Moment1 (a) and moment2 (b) maps of $H^{13}CO^+$ line transition. Filaments, along with their labels, are overplotted on the maps. The '+' marks are the locations of the dense cores. Both the moment maps are generated within velocity range of [-48.1, -29.7] km s^{-1} and considering pixels above 5σ, where $\sigma = 0.009$ Jy/beam. Scale bar and beam size are also shown on the maps.

moment 1: ガスの平均速度
moment 2: ガスの速度分散

ATOMS: ALMA Three-millimeter Observations of Massive Star-forming regions – XVII. High-mass star-formation through a large-scale collapse in IRAS 15394−5358

- ガス流入速度が中心のハブの速度分散と同じ(~ 2 km s^{-1})と仮定すると、質量降着率は3 x 10^{-3} M_{sun} yr^{-1}。
    - C-1の質量を自由落下時間(5 x 10^4 yr)の数倍で降着できる。 $\dot{\mathrm{M}}_{\mathrm{in}} = 3\mathrm{V}_{\mathrm{in}}^3/2\mathrm{G}$
    - global hierarchical collapseモデルによるcompetitive accretion(競争的降着?)と整合的か。
        - 初期に、分子雲がJeans core質量へ分裂した。
        - 最も質量の大きいコア(C-1)がハブに位置している。
        - 他の密度の高いコアC-2, C-3は、最も速度勾配の大きいフィラメントF4に位置している。

Giant planets population around B stars from the first part of the BEAST survey

- 大質量星であるB型星周りの惑星形成は、極限的環境という意味で重要。
- Scorpius-Centaurus associationにおける若いB型星(平均16 Myr)周りの巨大惑星の存在頻度を調べた。

Context. Exoplanets form from circumstellar protoplanetary discs whose fundamental properties (notably their extent, composition, mass, temperature and lifetime) depend on the host star properties, such as their mass and luminosity. B-stars are among the most massive stars and their protoplanetary discs test extreme conditions for exoplanet formation.
Aims. This paper investigates the frequency of giant planet companions around young B-stars (median age of 16 Myr) in the Scorpius-Centaurus association, the closest association containing a large population of B-stars.
Methods. We systematically search for massive exoplanets with the high-contrast direct imaging instrument SPHERE using the data from the BEAST survey, that targets an homogeneous sample of young B-stars from the wide Sco-Cen association. We derive accurate detection limits in case of non-detections.
Results. We found evidence in previous papers for two substellar companions around 42 stars. The masses of these companions are straddling the ~13 Jupiter mass deuterium burning limit but their mass ratio with respect to their host star is close to that of Jupiter. We derive a frequency of such massive planetary mass companions around B stars of 11^{+7}_{-5}%, accounting for the survey sensitivity.
Conclusions. The discoveries of substellar companions b Centauri b and μ^2 Sco B happened after only few stars in the survey had been observed, raising the possibility that massive Jovian planets might be common around B-stars. However our statistical analysis show that the occurrence rate of such planets is similar around B-stars and around solar-type stars of similar age, while B-star companions exhibit low mass ratios and larger semi-major axis.

- SPHEREのBEAST survey (B-star Exoplanet Abundance Study)の高コントラスト直接撮像を用いた。
  - 非検出の場合には検出限界を導出した。
- 42個の星の周りに2つのsubstellar companions (b Centauri b, μ^2 Sco B)を見つけた。
  - 質量は13木星質量(deuterium burning limit)に近いが、主星との質量比は木星のものに近かった。
  - B型星周りの巨大惑星の存在頻度は11^{+7}_{-5} %であった。
- substellar companionsの存在頻度は、B型星も太陽型星も同程度であることがわかった。
  - B型星のほうが質量比が低く、軌道長半径が大きい。

Giant planets population around B stars from the first part of the BEAST survey

- 星のサンプル:
  42→34個に減らしたが、
  減らした星も
  companionsはなかった。

Table 1. Sample of stars used for this study's statistical analysis.

Name	Age (Myr)	Mass ($M_\odot$)	Sp. type
HIP58452	20^{+5}_{-5}	3.0 ± 0.3	B8.5V
HIP58901	13^{+3}_{-3}	2.9 ± 0.3	B9V
HIP60009	12^{+4}_{-2}	6.5 ± 0.6	B2.5V
HIP60379	13^{+3}_{-3}	3.8 ± 0.4	B7V
HIP60823^{*1}	17^{+3}_{-3}	7.2 ± 0.7	B2V
HIP61585^{*1}	15^{+3}_{-3}	$9.8^{+1.1}_{-1.0}$	B2V
HIP62058	15^{+3}_{-3}	3.4 ± 0.3	B
HIP62327^{*1}	17^{+3}_{-3}	5.4 ± 0.5	B2.5V
HIP63003	16^{+3}_{-3}	7.1 ± 0.7	B2V
HIP65112	15^{+3}_{-3}	4.0 ± 0.4	B5V
HIP66454	17^{+3}_{-3}	4.0 ± 0.4	B8V
HIP67464^{*1}	18^{+3}_{-5}	8.2 ± 0.8	B2V
HIP67669^{*1}	17^{+3}_{-3}	4.8 ± 0.5	B5V
HIP67703	16^{+3}_{-3}	3.4 ± 0.3	B8V
HIP68245	17^{+3}_{-3}	7.9 ± 0.8	B2V
HIP68282^{*1}	21^{+4}_{-2}	6.6 ± 0.7	B2V
HIP69011	17^{+3}_{-3}	2.3 ± 0.2	B9.5V
HIP70300	17^{+3}_{-5}	5.9 ± 0.6	B2V
HIP70626	15^{+3}_{-3}	3.3 ± 0.3	B9V
HIP71352	15^{+3}_{-3}	9.7 ± 1.0	B2V
HIP71536^{*2}	14^{+4}_{-4}	6.2 ± 0.6	B3.5V
HIP71865^{*2}	14^{+3}_{-3}	5.9 ± 0.6	B2.5V
HIP74950^{*1}	18^{+3}_{-3}	4.4 ± 0.4	B7V
HIP76591	17^{+3}_{-3}	3.0 ± 0.3	B9V
HIP76600^{*1}	13^{+4}_{-3}	7.5 ± 0.7	B2.5V
HIP76633	7^{+3}_{-2}	2.4 ± 0.2	B9V
HIP77562	17^{+3}_{-3}	2.9 ± 0.3	B9V
HIP77968	17^{+5}_{-2}	3.4 ± 0.3	B8V
HIP78207	$0.5^{+0.5}_{-0.2}$	4.7 ± 0.5	B5V
HIP79044^{*1}	17^{+3}_{-3}	2.7 ± 0.3	B9V
HIP80911	16^{+4}_{-4}	8.8 ± 0.9	B2V
HIP82514^{*1}	20^{+4}_{-4}	10.0 ± 1.0	B1V
HIP82545	20^{+4}_{-4}	9.1 ± 0.3	B2V

Notes. * Star is a short separation (<0.1") binary. Binarity source : *1, from Gratton et al. (2023); *2, from Rizzuto et al. (2013) Spectral types are from Simbad.

- 検出した2つの惑星の軌道長半径 vs 質量/主星との質量比
  b Centauri b: 11±2 M_{Jup}, mass ratio 0.1–0.17%, 560 au
  μ^2 Sco B: 14±1 M_{Jup}, mass ratio < 0.2%, 290 au
- (1)系外惑星 < 13 M_{Jup}: 1検出
  (2)系外惑星・低質量褐色矮星(ELBD) < 30 M_{Jup}: 2検出
  (3)Substellar objects < 73.3 M_{Jup}: 2検出

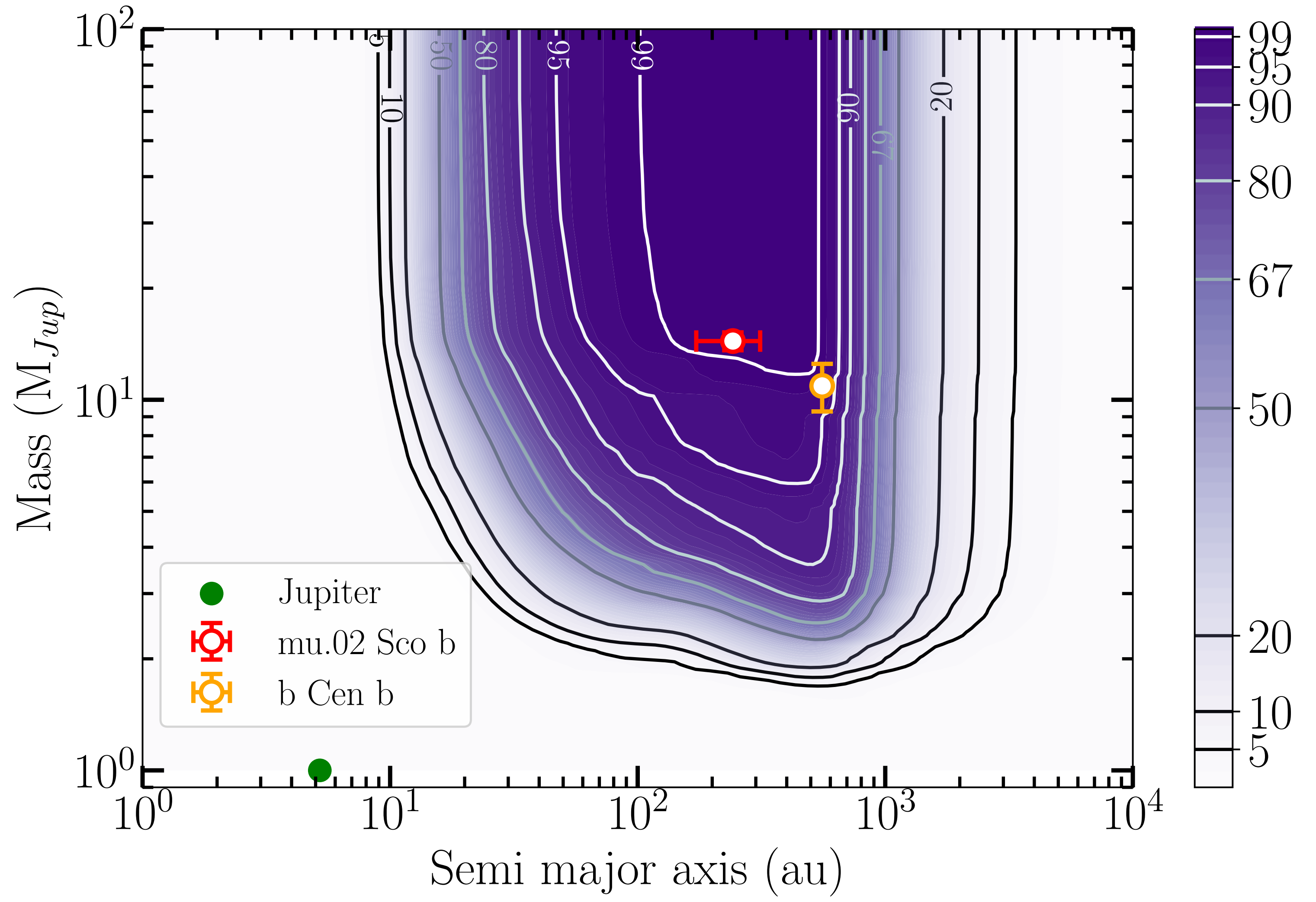

Fig. 5. Average detection probability of a companion of given mass/sma in the BEAST intermediary survey using the cond atmospheric model. The two detected planets in this survey are also represented with the mass / sma extracted from Janson et al. (2021a) and Squicciarini et al. (2021). Jupiter is also added to provide comparison. In the case of b Centauri b, no semi-major axis estimation is available, so we represented its projected separation.

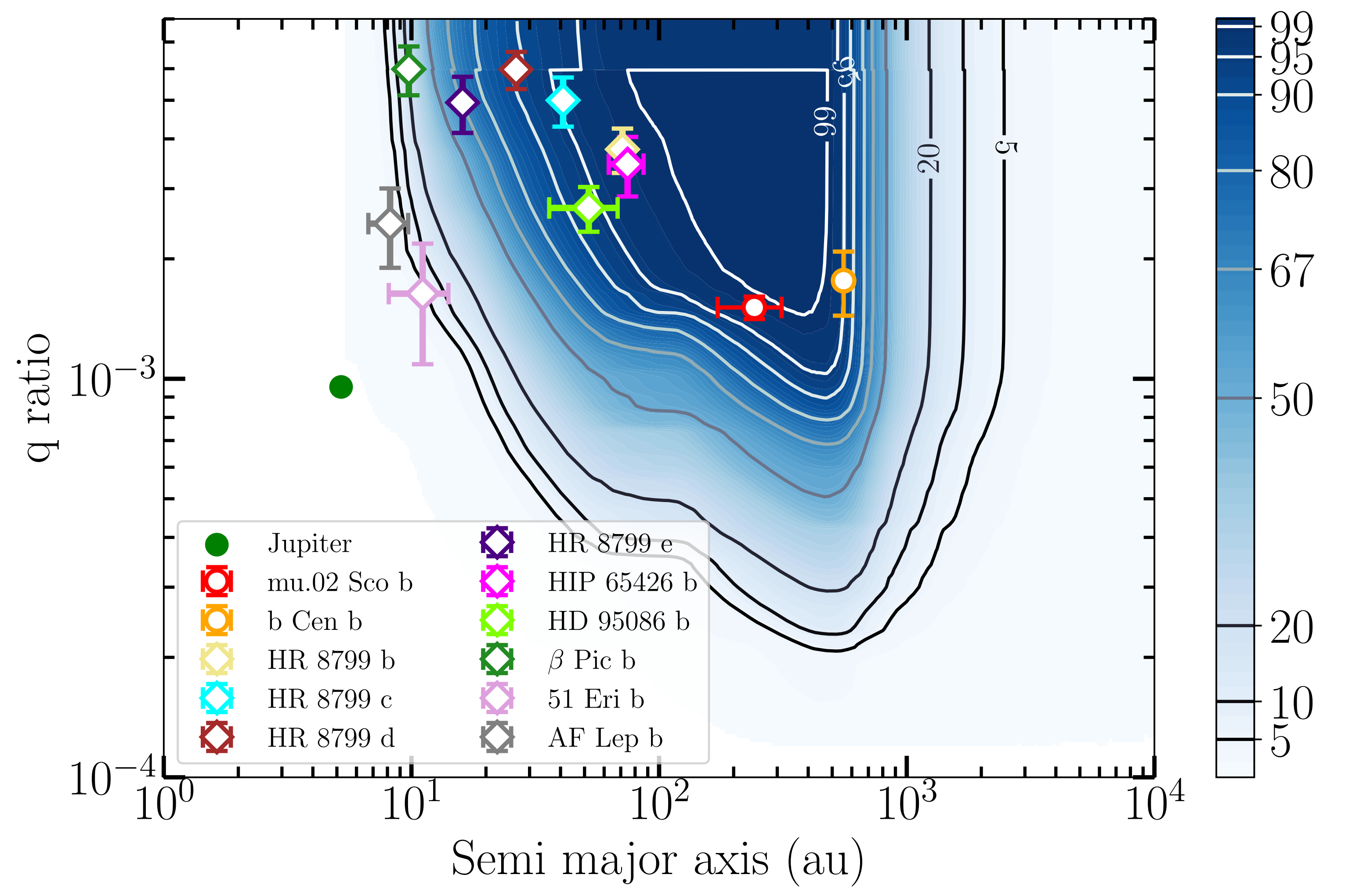

Fig. 6. Same as Figure 5 but expressed in companion to primary star mass-ratio. Several emblematic systems are added to the plot, **represented by the hollow diamonds**. Data are extracted from Zurlo et al. (2022) for HR 8799 bcde, Desgrange et al. (2022) for HD 95086 b, Blunt et al. (2023) for HIP 65426 b, Lagrange et al. (2020) for β Pictoris b, Brown-Sevilla et al. (2023) for 51 Eri b and Zhang et al. (2023) for AF Lep b.

Giant planets population around B stars from the first part of the BEAST survey

- 2–13 M_{Jup}, 10–1000 auの惑星の average survey sensitivity (or completeness): 64.1%
  - 34個のサンプル → 有効サンプル数21.8 (= 34 x 0.641)
  - 1つの系外惑星検出 → 存在頻度4.6%
- 2–30 M_{Jup}, 10–1000 auの惑星の average survey sensitivity (or completeness): 70.5%
  - 34個のサンプル → 有効サンプル数24 (= 34 x 0.705)
  - 2つのELBD検出 → 存在頻度8.5%
- ベイズ推定:

Table 3. Derived occurrence rates for companions within various mass ranges around our sample of B stars.

Occurrence :	Median	68% confidence	95% confidence
Exoplanet[1]	7.7%	[3.3–14.6]%	[1.1–24.3]%
ELBD [2]	11.0%	[5.8–18.4]%	[2.6–28.0]%
Substellar[3]	10.5%	[5.5–17.5]%	[2.5–26.7]%

Notes. [1]: <13M_{Jup}; [2]: <30M_{Jup}; [3]: <73.3 M_{Jup}

- 太陽型星とB型星周りのcompanion存在頻度の比較: あまり変わらない

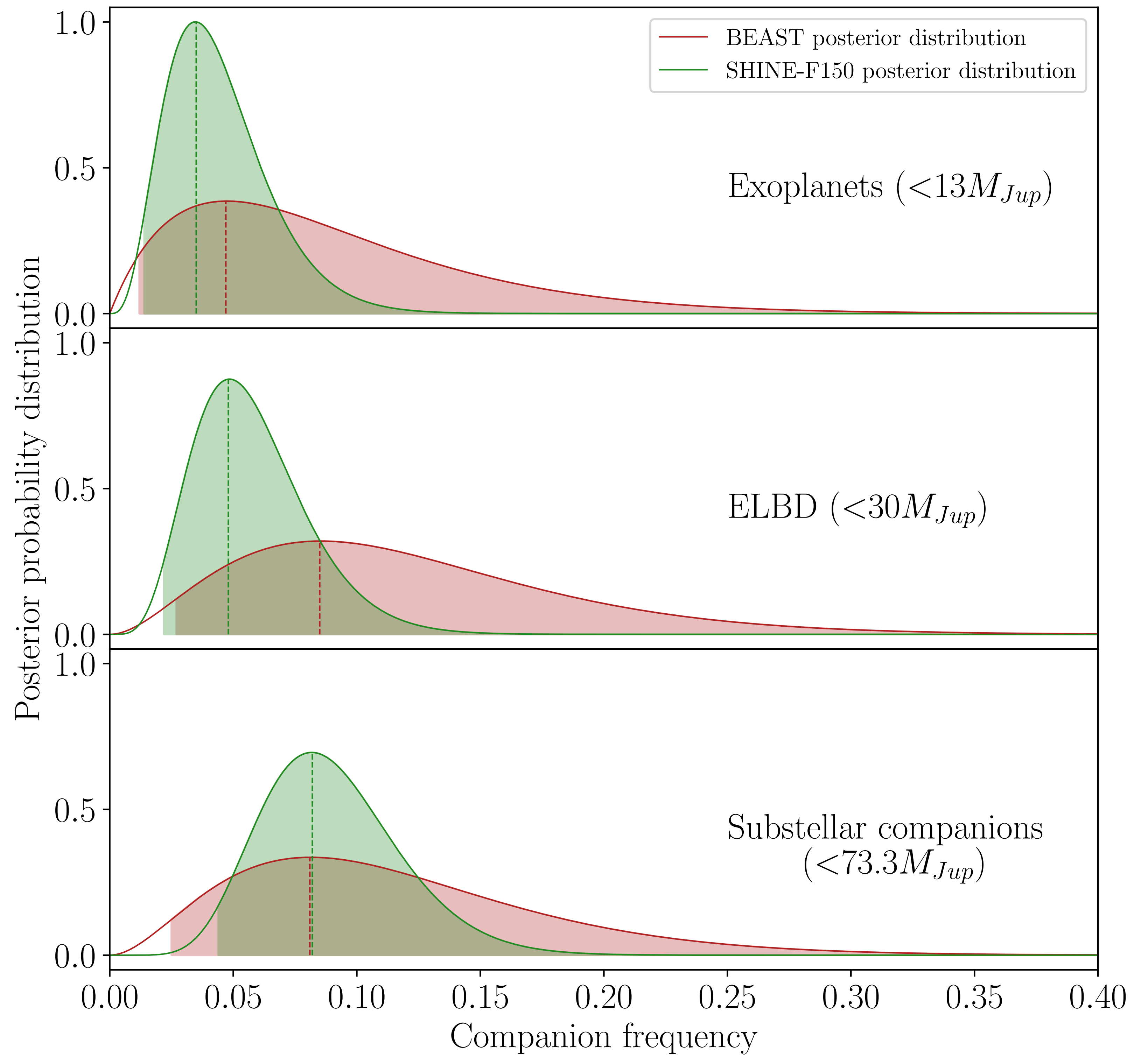

Fig. 7. Comparison of the normalised posterior distribution for the frequency of systems with at least one companion below a given mass, between the SHINE-F150 survey targeting mostly solar-type stars and the BEAST survey targeting only B stars.The shaded areas highlight the 95% confidence interval for each distribution and the vertical dashed line highlight the posterior maximum.

Giant planets population around B stars from the first part of the BEAST survey

- B型星周りでの系外惑星・低質量褐色矮星(ELBD)の形成過程: コア分裂、重力不安定、惑星捕獲、コア降着
    - 重力不安定: companionsはより大質量になる。2つのELBDsだけ観測したのと整合的でない。
        - 磁場を考慮すれば観測と一致するかもしれない。
    - コア分裂: 多重星や褐色矮星/系外惑星系を形成する。重力不安定と同様の問題を持つ。
    - コア降着: B型星のように熱く明るい星の周りの円盤光蒸発の非常に速いタイムスケールよりも、コア降着による巨大惑星形成のタイムスケールのほうが大きいという問題がある。
    - 惑星捕獲: 観測されたELBDの数を説明できない。
- どのシナリオもB型星周りの惑星数を説明できそうにない。